Optimum Design of Truss Structures with Active and Passive Damping Augmentation

R. A. Manning
TRW Space and Technology Group
Redondo Beach, California

ABSTRACT

This work is concerned with the development of an optimum design capability for truss structures augmented with active and passive members. The active members consist of piezoelectric sensors and actuators embedded within the layup of graphite epoxy composite members. The passive members consist of cocured viscoelastic material/graphite epoxy composite tubes. A two stage design optimization procedure is described which avoids the solution of the combinatoric optimization problem associated with active/passive member placement. A numerical example of a large complex space mission is included to demonstrate the feasibility of the design optimization procedure.

INTRODUCTION

New and innovative structural/control hardware and design techniques are necessary for the success of future space missions. The synergistic design application of passive damping will also aid in the elimination of harmful controls/structure interactions and model uncertainties.

Viscoelastically damped passive members [1] and active members with embedded piezoelectric sensors and actuators [2,3] have recently been fabricated and tested at the component level. These technologies suppress structural vibrations with minimal mass, complexity, and power consumption impact. The next step in the development of these technologies is the design and demonstration of the active and passive members at the system level. In order to do this, a simultaneous design procedure is needed.

Bronowicki and Diaz presented analysis and optimization techniques for constrained layer, viscoelastically damped members in Ref. 1. The techniques were applied to a single component which was then successfully fabricated and tested. A system level design optimization technique for

viscoelastic damping treatments based on the modal strain energy method was presented in Ref. 4. The method utilized a pre-packaged finite element method where behavior sensitivities were obtained semi-analytically.

Regarding active members, a number of previous studies have demonstrated integrated structure/control design methods using member actuators. An integrated optimization methodology for member actuators using direct output feedback was examined by Lust and Schmit [5]. Thomas and Schmit [6] advanced this idea and added dynamic stability constraints to insure convergence to a stable design for non-colocated sensors and actuators. McLaren and Slater [7] included various control compensators in their covariance approach to the integrated optimization problem. A useful finding of this latter work was the decrease in the value of the objective function as the order of the compensator is increased (see Figures 4 and 8, Ref. 7).

The work presented herein is concerned with the development of an integrated design optimization methodology where structural, passive member, active member, and control compensator design variables are treated simultaneously. Analytical mass and stiffness matrices, as well as mass and stiffness sensitivities, are obtained analytically by deriving these quantities at the element level. The integrated design process is intended for large complex structures where purely structural solutions or even sequential design solutions have little or no potential for success in meeting the stringent performance requirements. By including the compensator parameters in the optimization procedure, better performance can be obtained while meeting stability constraints than for direct output feedback.

SYSTEM DESCRIPTION

Many future space systems will consist of baseline truss structures from which reflectors, antennae, communications equipment, and electronics equipment are mounted. The work considered herein is concerned with truss structures augmented with passive and active members. It has been assumed that overall system performance can be derived from motions of specific points on the truss (e.g., sensitive optical components are hard-mounted to certain points on the structure).

The structural dynamic equations of motion can be written as

$$M\ddot{z} + [(1 + i\gamma^s)K^s + i\gamma^p K^p]z = R + bu \tag{1}$$

where M and K^s are the real mass and stiffness matrices, z is the vector of physical displacements, and R is the vector of externally applied nodal loads. Inherent damping in the inert truss is modeled as structural damping and enters the equations through the γ^s parameter. The passive damping members contribute to the standard real mass and stiffness matrices, but also add the complex damping term $i\gamma^p K^p$ [8]. Active members contribute

to the standard real mass and stiffness matrices, but also add the final term on the right hand side of equation (1). This final term consists of the b matrix locating actuators on the structure and the vector of actuator forces, u. Equation (1) can be written in state space form as

$$\dot{Z} = AZ + Bu \tag{2}$$

where undamped normal modes have been used to reduce the size of the matrices. The state vector, Z, is the stacked vector of modal displacements and velocities

$$Z = \left\{ \begin{array}{c} q \\ \dot{q} \end{array} \right\} \tag{3}$$

and the plant matrix, A, and input matrix, B, are given by

$$A = \left[\begin{array}{cc} 0 & I \\ -\omega^2 & -\phi^T \gamma^p K^p \phi - \phi^T \gamma^s K^s \phi \end{array} \right] \tag{4}$$

and

$$B = \left\{ \begin{array}{c} 0 \\ \phi^T b \end{array} \right\} \tag{5}$$

and ϕ is the matrix of normalized undamped modes.

A block diagram for the systems under study is shown in Figure 1. The plant (Box A) consists of inert truss members, concentrated masses, viscoelastically damped members, and the unenergized active members. Sensor measurements are available and are given by (Box B)

$$y = C_s Z + D_s u \tag{6}$$

where the C_s matrix locates sensors on the structure. Closing the local loops around the active members activates the compensator (Box D in Figure 1) which consists of the A_c, B_c, and C_c matrices. Compensator voltage degrees-of-freedom are given by

$$\dot{V} = A_c V + B_c y \tag{7}$$

The specific elements of each of the A_c and B_c matrices depend on the control law being used. In this work, either a third order Strain Rate Feedback (SRF) or a fourth or sixth order Positive Position Feedback (PPF) compensator was tied around each active member.

Closing the loops around the active members results from combining equations (2), (6), (7), and the feedback relation

$$u = -C_c V \tag{8}$$

to give

$$\dot{X} = \tilde{A} X + \tilde{B} u \tag{9}$$

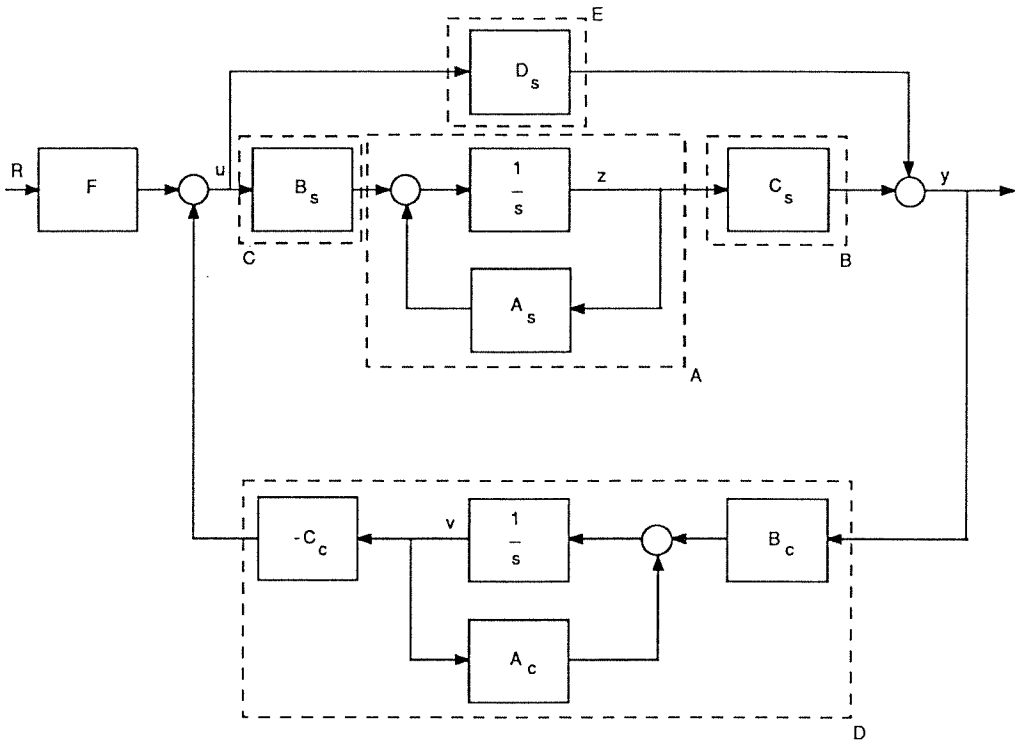

Figure 1: System Block Diagram

where the vector X includes both modal coordinates and compensator voltages. Solution of equations (9) in the frequency (or time) domain yields the closed loop system response.

The design variables and optimization variables for each type of element in the system are shown in Figure 2. For the inert truss members, the tube diameter and wall thickness were taken as design variables while the reciprocal of the cross sectional area was used as the optimization variables. For the passive members, the inside tube diameter and wall thickness, viscoelastic material thickness, and constraining layer thickness were the design variables. The optimization variables were chosen as the reciprocal of the areas of the inside tube, the viscoelastic material, and the constraining layer. For the active members, the inside dimension and wall thickness of the member were taken as design variables whereas the reciprocal of the area was used as the optimization variable. Design and optimization variables for the local compensator wrapped around each active member were the filter frequency and damping ratio and the overall compensator gain.

A mass penalty of 100% of the structural mass of the passive member was added to account for thermal control hardware. In addition, a mass penalty of 200% of the structural mass of the active member was added to

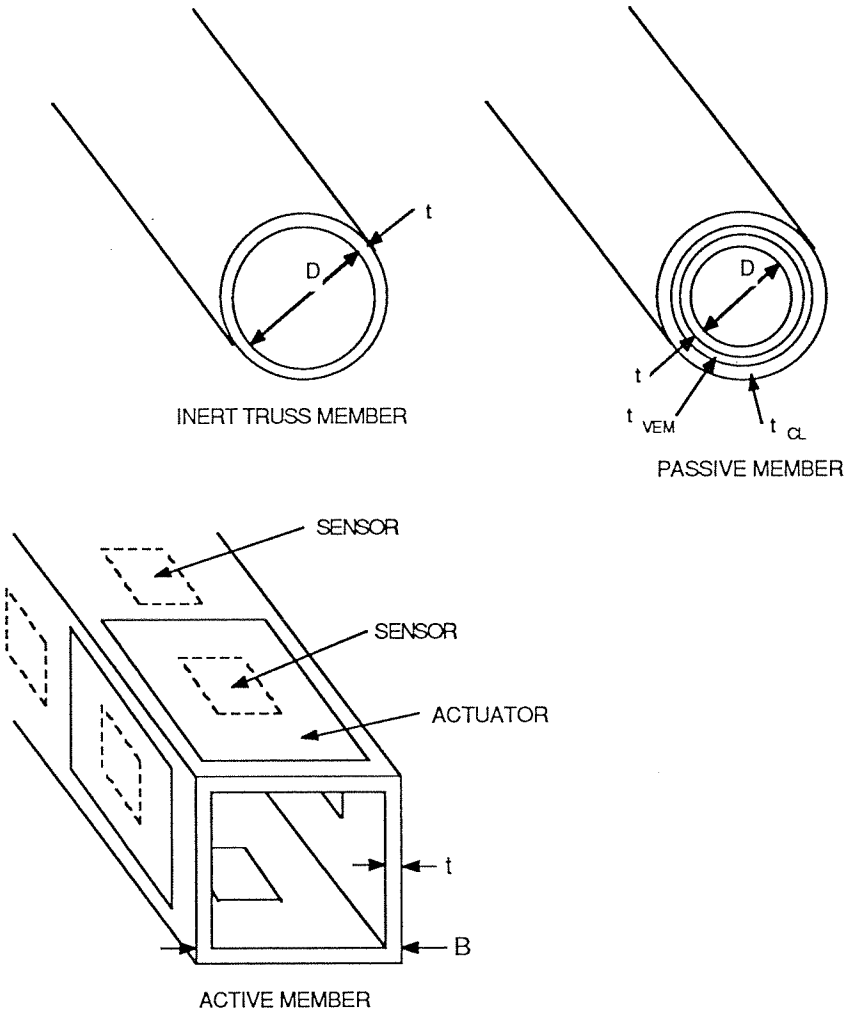

Figure 2: Design Element Details

account for thermal control, electronics, and power consumption hardware.

OPTIMUM DESIGN PROBLEM STATEMENT

For many space missions, a single performance index, such as line-of-sight (LOS) or pointing error, is the critical parameter for mission success. Minimization of this quantity maximizes system performance. However, additional constraints must be imposed on other quantities within the system. For example, line-of-sight may depend on the relative displacement and rotation of a number of optical elements within the system. The goal of the optimization process is to minimize LOS without allowing any of

the optical elements to exceed their range of motion or hit their mounting stops.

For such missions, the optimization problem can be stated as

$$\min \ \mathrm{LOS(d,f)} \tag{10}$$

subject to

$$g(d,f) \leq 0 \tag{11}$$

along with the side constraints

$$d^l \leq d \leq d^u \tag{12}$$

where it is understood that d is the vector of design variables for the inert truss members, passive damping members, and active members as discussed in the previous section.

In general, the design problem stated in equations (10) through (12) is an implicit nonlinear mathematical programming problem. Furthermore, embedded within the optimum design problem statement is the placement of the passive and active members on the structure. The placement aspect of the design problem requires a computationally burdensome combinatoric optimization solution technique. It can be stated from a computational experience viewpoint that the design problem posed in equations (10) through (12) defies attempts at a direct solution.

SOLUTION METHODOLOGY

In this work, the solution procedure for the optimum design problem stated in equations (10) through (12) is broken into a heuristic subproblem and a formal subproblem. A pictorial description of the complete solution sequence to the original optimum design problem is shown in Figure 3. In the heuristic subproblem, locations for the passive and active members are determined by examining regions of high strain energy for those modes which contribute most to the objective function and the constraints. Once the locations of the passive and active members have been found, a formal subproblem based on equations (10) through (12) is solved. The formal subproblem replaces the implicit problem posed in equations (10) through (12) with the explicit approximate problem

$$\min \ \tilde{\mathrm{LOS}}\mathrm{(d,f)} \tag{13}$$

subject to

$$\tilde{g}(d,f) \leq 0 \tag{14}$$

along with the side constraints

$$d^l \leq d \leq d^u \tag{15}$$

The $L\tilde{O}S$ and $\tilde{g}$ represent explicit first order Taylor series approximations for the objective function and constraints, respectively.

Solution of the implicit optimum design problem posed in equations (10) through (12) proceeds by solving a sequence of heuristic and formal subproblems. Each formal subproblem involves solving a sequence of approximate problems (stated in equations (13) through (15)).

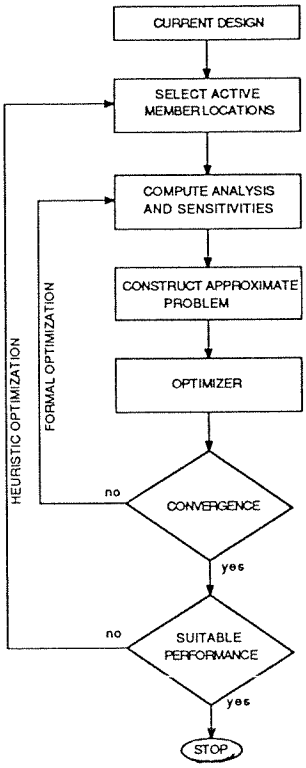

Figure 3: Solution Procedure Flow Diagram

EXAMPLE PROBLEM

An example problem is used to demonstrate the feasibility of the optimum design procedure. Figure 4 shows a potential concept for a Space Based Interferometer (SBI) [10]. The interferometer consists of an 11 meter tower with a telescope running down the center of it. Two 13 meter arms are attached at the base of the tower and support collecting telescopes at their tips. The 13 meter arms yield a baseline optical path length of 26 meters. Internal measurements are available from the laser metrology equipment mounted at the end of an 11 meter truss.

Maximum performance from the SBI is obtained when optical path length excursions from 26 meters are minimized during normal operations. Limited field of view of the collecting telescopes require tip and tilt of the telescopes to be below 5 μradians. A wide-band disturbance is applied at the central structure of the SBI to simulate reaction wheel out-of-balance

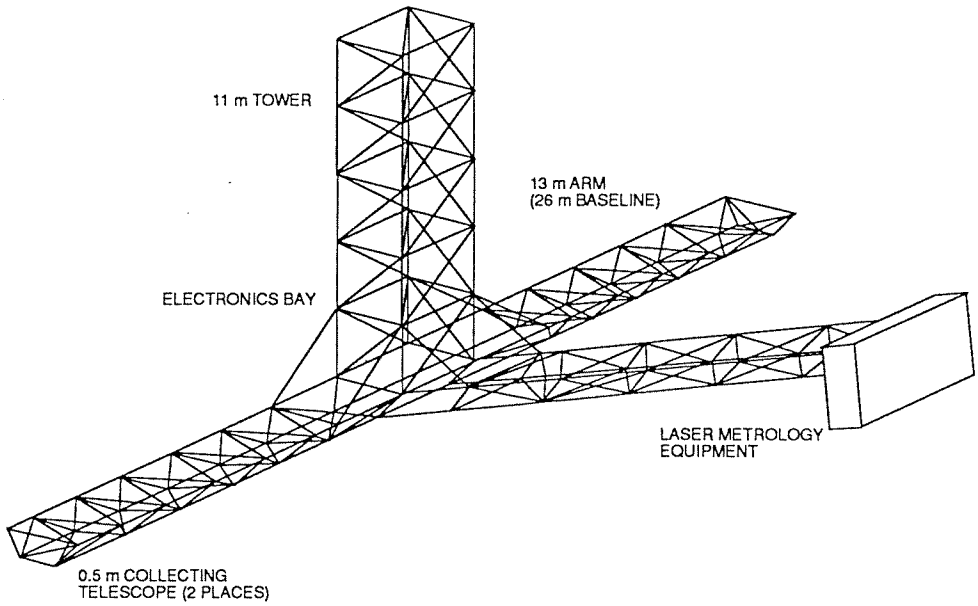

Figure 4: Space Based Interferometer Concept

and noise. The optimum design problem is to minimize optical path length excursions from 26 meters with upper bound constraints of 5 μradians on the relative tilt and tip of the collecting telescopes. An upper bound cap on the total system mass is also imposed to insure that the SBI is within the launch vehicle's capability for a given orbit.

The initial design of the SBI (with no active or passive damping augmentation) has a mass of 252 kgs. Strength and geometric considerations were used to arrive at sizes for the members. The initial mass of 252 kgs also serves as the upper bound mass cap during the optimization. The top traces of Figure 5 show the performance of the interferometer at the initial design. The modes at 7.2, 8.4, 16.4, 18.9, 27.7, and 36.8 Hz contribute to unacceptable optical lengths as well as relative tilt and tip motions of the collecting telescopes exceeding their bounds.

The heuristic subproblem for active and passive member locations was solved by placing these members in regions of high strain energy for the troublesome modes. Optimum values for the design variables were then found by solving the formal subproblem. Four to five approximate problem solutions were typically needed to achieve acceptable designs.

Table 1 gives the levels of damping that were obtained in each of the complex structural modes below 40 Hz as well as the values of the constraints and objective function. Fourteen active members and ten passive members with a total mass of 15 kgs were utilized in achieving these results. The bottom trace in Figure 5 shows the performance of the interferometer at the optimum design. The integrated design optimization methodology

achieved a factor of 40 improvement in SBI baseline while regaining feasibility with respect to telescope tilt and tip responses.

Table 1: Initial and Optimum Frequencies and Damping Ratios

	Initial Design		Optimum Design	
Mode Number	Frequency (Hz)	$\zeta(\%)$	Frequency (Hz)	$\zeta(\%)$
1-6	0.0	0.0	0.0	0.0
7	4.4	0.2	4.3	10.7
8	6.5	0.2	6.3	2.9
9	7.2	0.2	6.9	6.9
10	8.4	0.2	8.0	3.6
11	8.5	0.2	8.3	4.1
12	12.9	0.2	12.4	11.9
13	16.4	0.2	15.3	13.1
14	18.9	0.2	17.7	10.1
15	19.1	0.2	18.1	20.1
16	21.7	0.2	20.7	0.5
17	24.5	0.2	23.8	0.5
18	27.7	0.2	26.8	11.7
19	29.0	0.2	27.2	1.8
20	36.8	0.2	33.4	11.7
Mass (kgs)	252		252	
Tip (μrad)	21		4.8	
Tilt (μrad)	48		4.2	
Baseline(μm)	3.2		.08	

CONCLUDING REMARKS

A two stage heuristic/formal optimization procedure has been described for the design of trusses with active and passive damping augmentation. The heuristic subproblem is concerned with the placement of the active and passive members in efficient locations. The formal subproblem then "sizes" all of the design variables with the fixed active and passive member locations. Approximation concepts are used to yield optimum designs in relatively few complete structural dynamic analyses. The design methodology is an integrated procedure which treats all design variables simultaneously.

The simultaneous treatment of the design variables takes advantage of the synergy that exists between the disciplines. By designing damping into the system early in the design process, superior performance can be achieved when compared to retrofit damping and/or purely structural solutions. Damping is designed into the lower modes without destabilizing the

higher modes by designing the roll-off characteristics of the compensator at the same time as the structural characteristics.

REFERENCES

[1] Bronowicki, A.J. and Diaz, H.P., Analysis, Optimization, Fabrication and Test of Composite Shells with Embedded Viscoelastic Layers, Proceedings of Damping '89, West Palm Beach, Florida, February 8-10, 1989, pp. GCA-1-GCA-21.

[2] Bronowicki, A.J., Manning, R.A., and Mendenhall, T.L., TRW's Approach to Intelligent Space Structures, presented at the ASME Winter Annual Meeting, San Fransisco, California, December 13-15, 1989.

[3] Fanson, J.L., Blackwood, G.H., and Chu, C-C., Active-Member Control of Precision Structures, Proceedings of the AIAA/ASME/ASCE/AHS/ASC 30th Structures, Structural Dynamics, and Materials Conference, Mobile, Alabama, April 3-5, 1989, pp. 1480-1494.

[4] Gibson, W.C. and Johnson, C.D., Optimized Designs of Viscoelastic Damping Treatments, Proceedings of Damping '89, West Palm Beach, Florida, February 8-10, 1989, pp. DBD-1-DBD-23.

[5] Lust, R.V. and Schmit, L.A., Control-Augmented Structural Synthesis, AIAA Journal, Vol. 26, Jan. 1988, pp. 86-94.

[6] Thomas, H.L. and Schmit, L.A., Control Augmented Structural Synthesis with Dynamic Stability Constraints, Proceedings of the AIAA/ASME/ ASCE/AHS/ASC 30th Structures, Structural Dynamics, and Materials Conference, Mobile, Alabama, April 3-5, 1989, pp. 521-531.

[7] McLaren, M.D. and Slater, G.L., A Covariance Approach to Integrated Control/Structure Optimization, Proceedings of the 31st AIAA Dynamics Specialists Conference, Long Beach, California, April 5-6, 1990, pp. 189-205.

[8] Hedgepeth, J.M. and Mobren, M., Investigation of Passive Damping of Large Space Truss Structures, Proceedings of Damping '86.

[9] Fanson, J.L. and Caughey, T.K., Positive Position Feedback Control for Large Space Structures, Proceedings of the 28th AIAA Dynamics Specialists Conference, Monterey, California, April 9-10, 1987, pp. 588-598.

[10] Laskin, R.A., A Spaceborne Optical Interferometer: The JPL CSI Mission Focus, Proceedings of the NASA/DoD Controls-Structures Interaction Technology Conference, NASA CP 3041, San Diego, California, January 29-February 2, 1989, pp. 1-16.

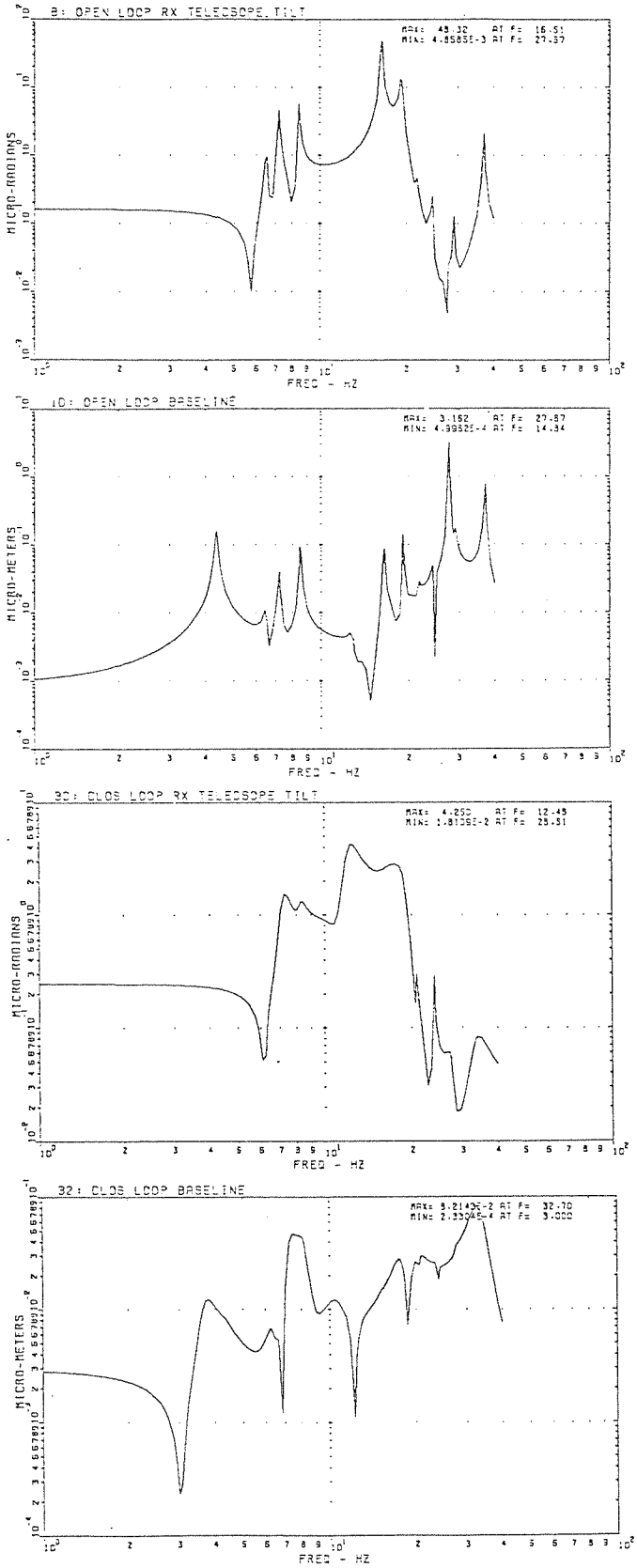

Figure 5: Initial and Final Baseline Response